

# The identification of a transposon affecting the asexual reproduction of the wheat pathogen *Zymoseptoria tritici*

Wang, Chen; Milgate, Andrew; Solomon, Peter S.; McDonald, Megan

DOI:

[10.1111/mpp.13064](https://doi.org/10.1111/mpp.13064)

License:

Creative Commons: Attribution-NonCommercial (CC BY-NC)

*Document Version*

Publisher's PDF, also known as Version of record

*Citation for published version (Harvard):*

Wang, C, Milgate, A, Solomon, PS & McDonald, M 2021, 'The identification of a transposon affecting the asexual reproduction of the wheat pathogen *Zymoseptoria tritici*', *Molecular Plant Pathology*, vol. 22, no. 7, pp. 800-816. <https://doi.org/10.1111/mpp.13064>

[Link to publication on Research at Birmingham portal](#)

## General rights

Unless a licence is specified above, all rights (including copyright and moral rights) in this document are retained by the authors and/or the copyright holders. The express permission of the copyright holder must be obtained for any use of this material other than for purposes permitted by law.

- Users may freely distribute the URL that is used to identify this publication.
- Users may download and/or print one copy of the publication from the University of Birmingham research portal for the purpose of private study or non-commercial research.
- User may use extracts from the document in line with the concept of 'fair dealing' under the Copyright, Designs and Patents Act 1988 (?)
- Users may not further distribute the material nor use it for the purposes of commercial gain.

Where a licence is displayed above, please note the terms and conditions of the licence govern your use of this document.

When citing, please reference the published version.

## Take down policy

While the University of Birmingham exercises care and attention in making items available there are rare occasions when an item has been uploaded in error or has been deemed to be commercially or otherwise sensitive.

If you believe that this is the case for this document, please contact [UBIRA@lists.bham.ac.uk](mailto:UBIRA@lists.bham.ac.uk) providing details and we will remove access to the work immediately and investigate.

# The identification of a transposon affecting the asexual reproduction of the wheat pathogen *Zymoseptoria tritici*

Chen Wang <sup>1</sup> | Andrew W. Milgate <sup>2</sup> | Peter S. Solomon <sup>1</sup> | Megan C. McDonald <sup>1,3</sup>

<sup>1</sup>Division of Plant Sciences, Research School of Biology, The Australian National University, Canberra, ACT, Australia

<sup>2</sup>NSW Department of Primary Industries, Wagga Wagga Agricultural Institute, Wagga Wagga, NSW, Australia

<sup>3</sup>School of Biosciences, University of Birmingham, Edgbaston, Birmingham, UK

## Correspondence

Megan C. McDonald and Peter S. Solomon, Division of Plant Sciences, Research School of Biology, The Australian National University, Canberra, ACT, Australia. Emails: m.c.mcdonald@bham.ac.uk (M. C. M.); peter.solomon@anu.edu.au (P. S. S.)

## Funding information

China Scholarship Council; Grains Research and Development Corporation; Australian National University

## Abstract

*Zymoseptoria tritici*, the causal agent of Septoria tritici blotch, is a fungal wheat pathogen that causes significant global yield losses. Within *Z. tritici* populations, quantitative differences in virulence among different isolates are commonly observed; however, the genetic components that underpin these differences remain elusive. In this study, intraspecific comparative transcriptomic analysis was used to identify candidate genes that contribute to differences in virulence on the wheat cultivar WW2449. This led to the identification of a multicopy gene that was not expressed in the high-virulence isolate when compared to the medium- and low-virulence isolates. Further investigation suggested this gene resides in a 7.9-kb transposon. Subsequent long-read sequencing of the isolates used in the transcriptomic analysis confirmed that this gene did reside in an active Class II transposon, which is composed of four genes named *REP9-1* to *-4*. Silencing and overexpression of *REP9-1* in two distinct genetic backgrounds demonstrated that its expression alone reduces the number of pycnidia produced by *Z. tritici* during infection. The *REP9-1* gene identified within a Class II transposon is the first discovery of a gene in a transposable element that influences the virulence of *Z. tritici*. This discovery adds further complexity to genetic loci that contribute to quantitative virulence in this important pathogen.

## KEYWORDS

effector, quantitative virulence, transcriptomics, transposon, wheat, *Zymoseptoria tritici*

## 1 | INTRODUCTION

The fungal wheat pathogen *Zymoseptoria tritici* is the causal agent of Septoria tritici blotch (STB). STB is one of the most devastating wheat diseases in Europe and is responsible for significant yield losses globally (O'Driscoll et al., 2014). While 22 qualitative "large effect" STB resistance genes have been mapped in bread wheat, no commercial wheat lines are fully resistant to all *Z. tritici* isolates (Brown et al., 2015; Yang et al., 2018). In addition to these named STB genes, there are over 160 "minor effect" quantitative trait loci

(QTLs) associated with STB resistance (Brown et al., 2015). While genetic resistance is used in the field, foliar-applied fungicide remains the primary method used to control the disease (Fones & Gurr, 2015; Torriani et al., 2015). However, fungicide resistance has been reported in nearly all areas where *Z. tritici* is a significant disease (Brunner et al., 2008; Estep et al., 2015; McDonald, Renkin, et al., 2019). This emerging resistance poses a significant threat to future wheat yields.

*Z. tritici* is a latent necrotroph, highly pathogenic on wheat leaves (Rudd et al., 2015; Sánchez-Vallet et al., 2015). To initiate

This is an open access article under the terms of the Creative Commons Attribution-NonCommercial License, which permits use, distribution and reproduction in any medium, provided the original work is properly cited and is not used for commercial purposes.

© 2021 The Authors. *Molecular Plant Pathology* published by British Society for Plant Pathology and John Wiley & Sons Ltd.

infection, spores of *Z. tritici* germinate on the surface of the leaf and the growing hyphae enter through stomata (Orton et al., 2011; Rudd et al., 2015). *Z. tritici* has a long, symptomless latent period that ranges from 8 to 14 days, depending on specific wheat cultivar–*Z. tritici* isolate combinations and other environmental factors (Keon et al., 2005, 2007; Rudd et al., 2015). After this symptomless stage, the mesophyll of infected leaves rapidly collapses, which manifests as large necrotic lesions. The fungus then sporulates, forming asexual fruiting structures called pycnidia (Orton et al., 2011). These pycnidia mature and the asexual spores, known as pycnidiospores, ooze out onto the leaf surface and are subsequently splash dispersed up the canopy, furthering the field epidemic (Suffert et al., 2011).

The disease symptoms caused by *Z. tritici* infection have primarily been described as a quantitative trait and significant effort has gone into automated tools that can quantify the extent of leaf necrosis or formation of pycnidia (Karisto et al., 2018; Stewart et al., 2017; Stewart & McDonald, 2014). In this work we define virulence genes as those that affect the extent or severity of disease symptoms (Agrios, 2005). In plant pathology, the term “aggressiveness” is often used instead of virulence to indicate the severity of disease symptoms (Bos & Parlevliet, 1995; Thomas & Elkinton, 2004). However, most studies on *Z. tritici* have adopted the term “virulence,” which more closely aligns with how the term is defined in other disease systems outside of plant pathology (Stewart et al., 2017). Despite the characterization of STB as a quantitative disease, recent studies have identified genes that qualitatively impact the STB disease outcome (Lee et al., 2014; Marshall et al., 2011; Zhong et al., 2017). *AvrStb6* is the first avirulence (*Avr*) gene cloned in *Z. tritici* and its expression leads to an avirulent phenotype on *Stb6*-containing wheat lines (Kema et al., 2018; Zhong et al., 2017). However, more studies have demonstrated or identified genes that have a quantitative effect on virulence. For example, in a large QTL study one locus, later identified as the gene *Avr3D1*, was shown to quantitatively influence both lesion size and pycnidia formation (Meile et al., 2018; Stewart et al., 2017). *Avr3D1* is unique because it interacts in a gene-for-gene manner with wheat cultivars that contain the *Stb7* resistance gene, but its expression and recognition do not abolish pathogen infection (Meile et al., 2018). Similarly, Poppe et al. (2015) identified three quantitative virulence-related genes in an interspecific resequencing study. In this study, the deletion mutants  $\Delta Zt80707$  and  $\Delta Zt103264$  showed reduced pycnidia formation on infected wheat leaves compared to the wild-type (WT) *Z. tritici* isolate IPO323, while  $\Delta Zt89160$  strains showed a hypervirulent phenotype with enhanced pycnidia formation during infection (Poppe et al., 2015). Together, these studies demonstrate that while single genes of large (qualitative) effect exist in the pathogen's genome, genes of smaller (quantitative) effect make significant contributions to disease development. When scaled to the field level, these small effect genes can play large roles in the speed and intensity of epidemic development and have a significant impact on yield.

The extended duration of the symptomless period of *Z. tritici* is unique in comparison to other necrotrophic wheat pathogens. Therefore, this latent period was the focus of several RNA-sequencing

(RNA-Seq) studies that sought to characterize putative virulence genes expressed during this stage (Hauelsen et al., 2019; Kellner et al., 2014; Palma-Guerrero et al., 2017; Rudd et al., 2015). Transcriptomic data from these studies suggest that *Z. tritici* actively reprogrammes its gene expression when transitioning from the latent to necrotic stages of infection. While these studies have provided significant insight into the complex changes *Z. tritici* undergoes during infection, only one study has specifically addressed quantitative differences in virulence between isolates infecting the same wheat cultivar (Palma-Guerrero et al., 2017). We sought to build upon our understanding of the genes underpinning virulence in *Z. tritici*, by assessing the transcriptome of three isolates with different levels of virulence on a single wheat cultivar. The transcriptomic profiles of these three isolates were compared in order to identify candidate genes that could be responsible for different degrees of virulence.

## 2 | RESULTS

### 2.1 | Three Australian *Z. tritici* isolates differ in virulence on wheat cultivar WW2449

In a previous screen on wheat, *Z. tritici* isolates WAI332, WAI323, and WAI321 showed different degrees of virulence on the wheat cultivar WW2449 (McDonald et al., 2016). This study relied on a visual scoring of disease severity from 1 to 5; however, newer tools developed within the community enabled more precise measurements of the differences in virulence between these three isolates (Karisto et al., 2018). To expand upon this result, the third leaves on WW2449 were infiltrated with each isolate and the disease was assessed at 14 to 21 days postinoculation (dpi). Consistent with the previous study, all three isolates caused necrotic lesions on WW2449 leaves; however, there were measurable differences in the number of pycnidia each isolate produced. At 21 dpi, abundant pycnidia were visible on WW2449 leaves infected with WAI321 followed by fewer pycnidia in leaves infected with WAI323 (Figure 1a). In contrast, pycnidia were almost absent on WAI332-infected leaves (Figure 1a). For clarity, we refer to these isolates by their virulence on WW2449 throughout the rest of the manuscript (WAI321, high virulence; WAI323, medium virulence; WAI332, low virulence).

Consistent with the previous visual assessment of pycnidia number, automated image analysis revealed that the high-virulence isolate WAI321 developed significantly more pycnidia per leaf, with an average of 21.2 pycnidia per infiltrated leaf. This is compared to an average of 5.2 pycnidia per infiltrated leaf for the medium-virulence isolate WAI323 (Figure 1b). Almost half of the low-virulence isolate WAI332-infected leaves showed no pycnidia with an average of only 2.5 pycnidia per leaf (Figure 1b). Pycnidia density (pycnidia per cm<sup>2</sup> necrotic lesion) was also assessed, where the same trend was observed (Figure 1c). No differences in total necrotic area between the three isolates was observed. These data confirm these isolates exhibit quantitative differences in their virulence, defined here as the ability to form pycnidia on the cultivar WW2449.

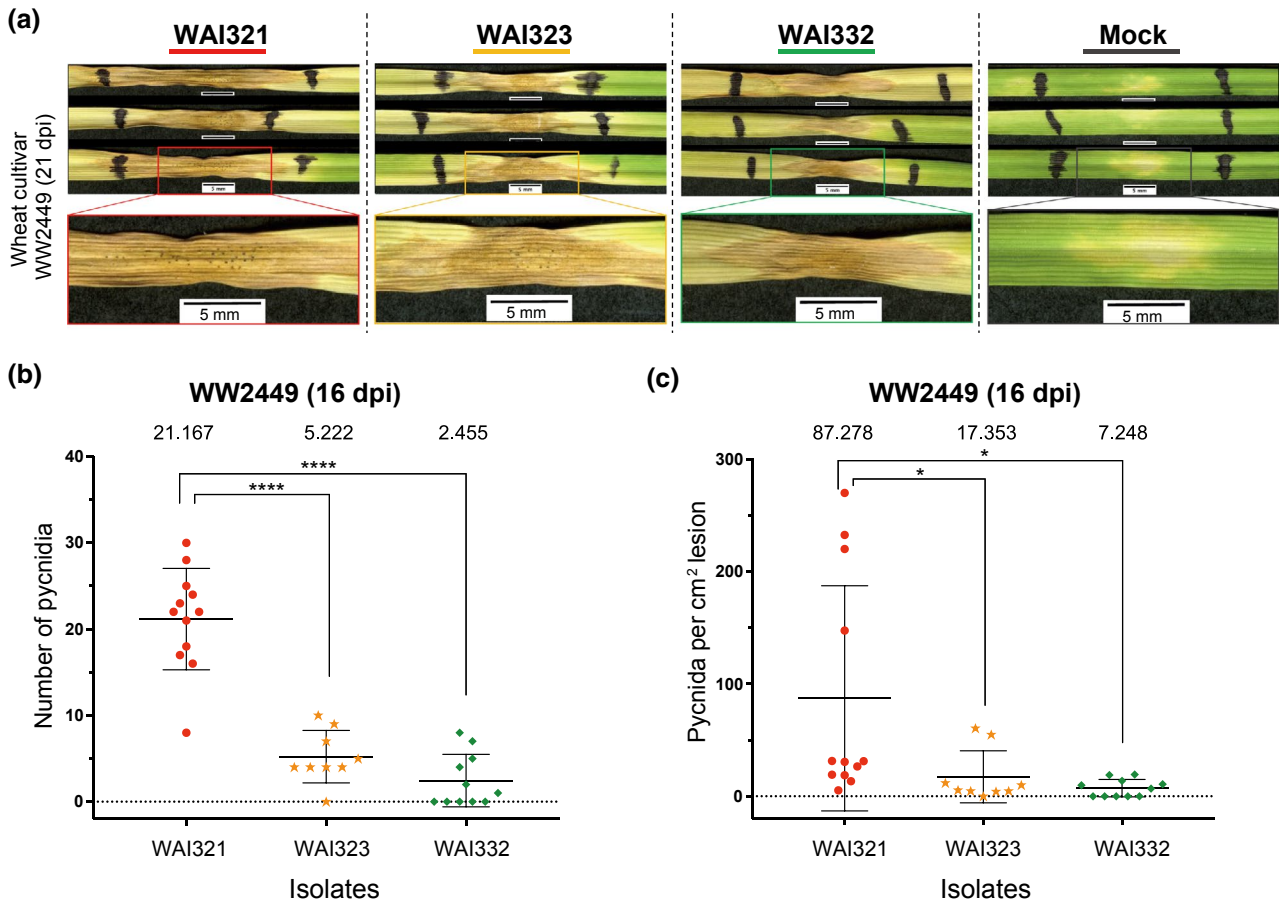


**FIGURE 1** Three Australian *Zymoseptoria tritici* isolates showing different degrees of virulence on the wheat cultivar WW2449. (a) The third leaves of the wheat cultivar WW2449 (infiltrated with *Z. tritici* isolates WAI321, WAI323, and WAI332) harvested at 21 days postinoculation (dpi). (b) The number of pycnidia produced on WW2449 leaves inoculated with WAI321, WAI323, and WAI332 counted at 16 dpi. Each infection assay was repeated twice and at least nine leaves were collected per isolate in each experiment. (c) Pycnidia density (pycnidia per cm<sup>2</sup> lesion) calculated based on the number of pycnidia and the area of necrotic lesions. All data in (b) and (c) passed the D'Agostino–Pearson normality test (omnibus K2 test); analysis of variance was conducted with the post hoc Tukey multiple comparisons test. Each dot represents an individual leaf sample; numbers on top represent the mean of each group; bars indicate  $\pm$ SD; \* $p < .05$ , \*\* $p < .01$ , \*\*\* $p < .001$ , \*\*\*\* $p < .0001$

## 2.2 | The three isolates have distinct transcriptomic profiles during infection

To identify genes facilitating pycnidia development in planta, RNA was extracted from infected WW2449 leaves before symptom development (9 dpi) and at the onset of the switch to necrotic growth (14 dpi) and sequenced. The total aligned reads were then counted, normalized, and subsequently used to construct a multidimensional scaling plot (MDS) to compare global transcript expression between samples (Figure 2a). This analysis showed tight clustering of the biological replicates, indicating suitable consistency between replicates and a clear separation of the different isolates from each other (Figure 2a). This suggests that each isolate has a distinct transcriptomic profile during infection on the cultivar WW2449. The MDS plot also revealed a clear separation in total transcript expression between 9 and 14 dpi for the more virulent isolates, WAI321 and WAI323. In contrast, there was little variation in gene expression

between the two time points for the weakly virulent WAI332 isolate (Figure 2a).

To focus the downstream analyses on differences between the isolates, three sets of differentially expressed genes (DEGs) were identified based on pairwise comparisons ( $p < .05$ , false discovery rate [FDR]  $< .05$ ,  $|\log_2$  fold-change (FC)  $\geq 1$ ). Due to the tight clustering of total gene expression in the low-virulence isolate WAI332 at both 9 and 14 dpi, we chose to analyse differential gene expression between the isolates only. Therefore, samples from different time points were treated in silico as replicates for this statistical analysis. The numbers of overlapping DEGs between pairwise comparisons are shown in Figure 2b. Overall, The WAI323/WAI332 (medium/low virulence) comparison showed the largest number of DEGs (1,967 DEGs, 13.06% of all annotated genes), while the WAI321/WAI332 (high/low virulence) comparison showed 1,259 DEGs (8.36% of all annotated genes; Figure 2b). In contrast, the WAI321/WAI323 pair showed only 498 DEGs (3.31% of all annotated genes), less than

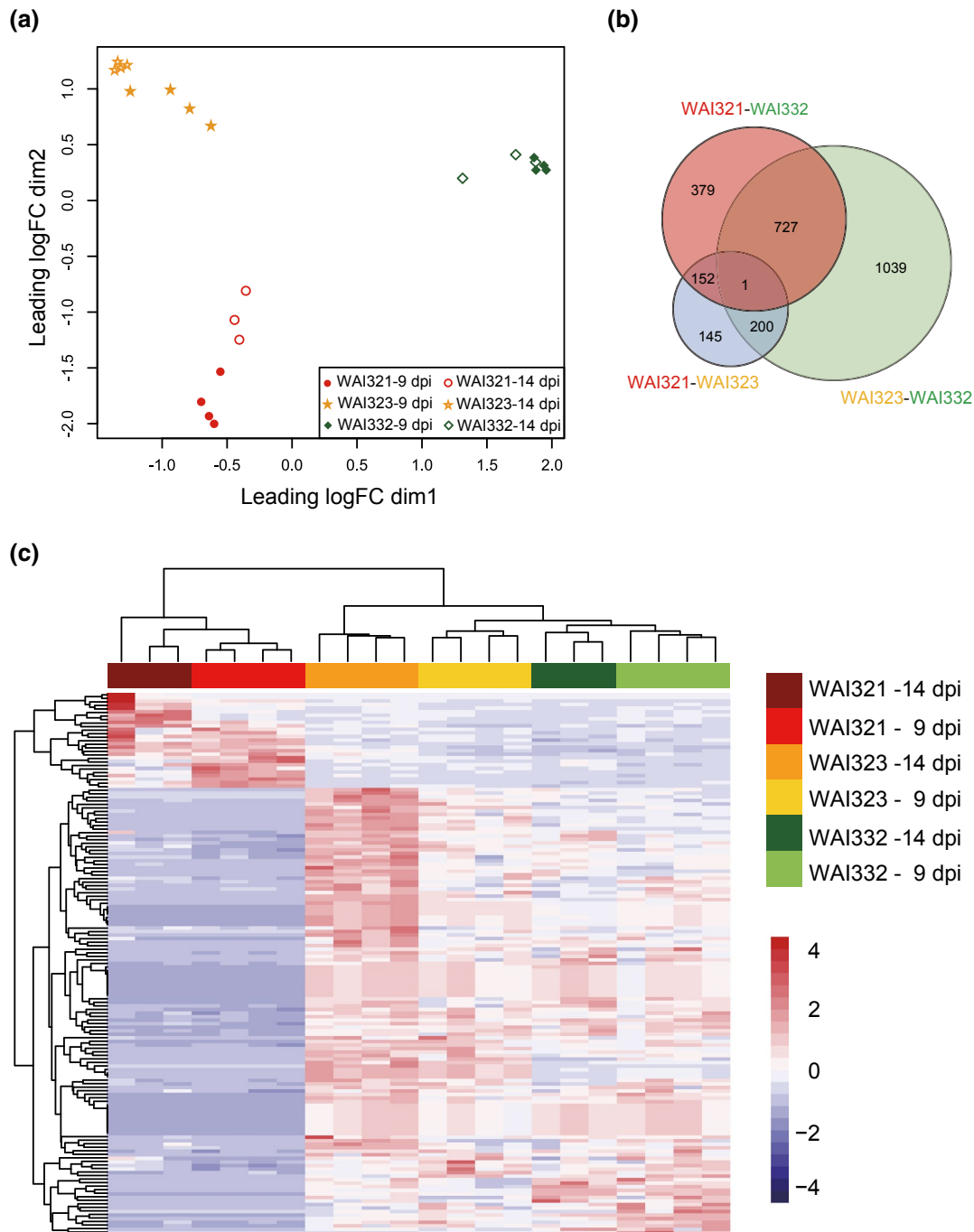


**FIGURE 2** Isolate-specific transcriptome analysis. (a) Multidimensional scaling (MDS) analysis using all normalized expression counts of the three isolates during infection on WW2449. The distance between each dot (sample label) indicates similarity. Dimension 1 (dim1) separates the isolates, whereas dimension 2 (dim2) roughly separates the days postinoculation (dpi). (b) Venn diagram showing the overlap of differentially expressed genes (DEGs) in WAI321–WAI332, WAI321–WAI323, and WAI323–WAI332 comparisons. DEG lists were generated using the criteria false discovery rate (FDR) < .05,  $p < .05$  and  $|\log_2 \text{fold-change (FC)}| \geq 1$ . (c) Heatmap (with cluster dendrogram) showing the expression profiles of the 153 WAI321-specific DEGs associated with the three *Zyloseptoria tritici* isolates. Colour legend indicates  $\log_{10}(\text{CPM} + 0.01)$ , with red indicating higher counts-per-million (CPM) values and blue CPM values as they approach zero

a quarter of the total DEGs from the other pairwise comparisons. These results suggest that the more virulent isolates WAI321 and WAI323 have more similar gene expression profiles during infection on WW2449 when compared to the low-virulence isolate WAI332 (Figure 2b).

### 2.3 | Identification of new virulence-related gene candidates in the DEGs

Based on the above phenotyping and RNA-Seq analysis, we chose to focus on the DEGs specific to the high-virulence isolate, WAI321.

Taking the intersection of the WAI321/WAI332 and WAI321/WAI323 DEGs, 153 DEGs were shared between these two groups (Figure 2b; Table S1). The expression patterns of these 153 DEGs for all samples are shown in Figure 2c. Strikingly, the majority of these genes were down-regulated in the high-virulence isolate WAI321 when compared to WAI332/WAI323 (Figure 2c; Table S1). This suggested that the virulence of isolate WAI321 may be driven by the down-regulation of certain genes during infection.

To further resolve this list, we used EffectorP to identify putative effector candidates (Sperschneider et al., 2016, 2018). This limited the number of differentially expressed effector candidates to only 28 genes (Table 1). We hypothesized that these 28 differentially expressed effector candidates may contribute to the virulence of WAI321 and are responsible for this isolate's increased ability to sporulate on cultivar WW2449. Table 1 shows the 28 differentially expressed effector candidates in comparisons of WAI321 with WAI323 and WAI332 (sorted by gene ID). All the genes in this table are on core chromosomes (Chr01–13) and most of them encode small hypothetical/unnamed proteins containing more than two cysteines. Of the 28 DEGs, 24 were down-regulated and only 4 were up-regulated in WAI321 during infection when compared to the other two isolates.

Upon further inspection of this list, one gene, *Chr01.828*, was found to be identical to eight other genes found in different locations throughout the genome (named *Chr01.1012*, *Chr01.1158*, *Chr03.150*, *Chr04.1008*, *Chr09.51*, *Chr09.795*, *Chr11.123*, and *Chr11.560*; these additional eight genes are not shown in Table 1). The *Chr01.828* gene has nine identical copies in the WAI332 genome and is predicted to encode a 193-amino acid protein that contains six cysteines. This gene was not expressed at detectable levels in WAI321 (high virulence) and only moderately expressed in both WAI323 and WAI332 (Figure S1; Table S1).

## 2.4 | A multicopy differentially expressed gene resides in a Class II transposon

The high number of copies of *Chr01.828* indicated that this gene might be a part of a transposon within the genome of WAI332. In close proximity to this gene were three other genes, *Chr01.829*, *Chr01.830*, and *Chr01.831*. Local BLASTn searches of the WAI332 genome assembly revealed that these three genes were colocalized with *Chr01.828* at all nine locations in the WAI332 genome. This region plus several hundred base pairs on either side of the genes was extracted and aligned. This alignment revealed distinct breakpoints that defined the boundaries of the high-identity region (c.96.3% pairwise identity). In total, this region spanned 7.9 kb and included four predicted genes. This 7.9-kb region was designated ZtREP9 (hereafter called REP9; Figure 3a), to reflect the nine copies found on five different chromosomes in the genome of WAI332. A self-alignment of the REP9 region revealed terminal inverted repeats (TIRs; Figure 3b), typical of Class II transposons (Wicker et al., 2007). The differentially expressed effector

candidate gene (*Chr01.828*) is the first gene in this region and was subsequently named REP9-1 (Figure 3a).

To further investigate these four genes we conducted an expression experiment in vitro, to test if the expression pattern of these genes was similar to the patterns observed in planta from the RNA-Seq experiment. In the REP9 element all genes, excluding REP9-1, were expressed in vitro in all three isolates (Figure 3c–f). However, during infection, REP9-2 was not expressed in any isolate (Figure S1a; Table S2). REP9-3 and REP9-4 were expressed in all the three isolates during infection (Figure S1b,c; Table S2). REP9-1 was not expressed at detectable levels in the high-virulence isolate WAI321 under in vitro conditions or in planta (Figures 3c and S1d; Table S2). In comparison, REP9-1 was expressed in both WAI332 and WAI323 under both conditions (Figures 3c and S1d; Table S1).

In order to explore the possibility that REP9 was a transposon, the four proteins encoded by the genes within REP9 were subjected to NCBI BLASTp (nr database) and PHYRE2 in silico structural prediction. All four are hypothetical proteins based on the BLASTp results. Notably, REP9-1 showed only four hits and REP9-3 showed no significant hits when excluding the *Zymoseptoria* genus from the BLASTp database (Table S3). Both REP9-1 and REP9-2 contain the DUF3716 domain of unknown function, and BLASTp hits to many other fungal species that have genes encoding this domain were found (Table S3). REP9-4 was the only gene that showed low similarity with other functionally annotated proteins. This included low amino acid similarity to an integrase core domain-containing protein (Table S3). PHYRE2 intensive modelling suggested that REP9-4 has high structural similarity (confidence score > 98%) to viral integrases/transposases that have available structure information (Supp. "Supp-REP9\_PHYRE2\_report.pdf" Dataset online). PHYRE2 analysis of REP9-1, REP9-2, and REP9-3 did not identify any high-confidence structural similarities. BLASTn results of the full REP9 sequence on the available genomes in the JGI MycoCosm database indicated that REP9 is only present in the *Zymoseptoria* genus (Table S4).

To further investigate REP9-4's structural similarities with known integrases/transposases, all known transposons available in RepBase were downloaded and BLASTp was used to identify any similar proteins (minimum query coverage, 90 amino acids; pairwise amino acid identity > 20%). We also constructed local BLASTn databases for the four sister species of *Z. tritici*, whose genomes are also available (Feurtey et al., 2020). The full REP9 transposon was found in all four sister species; however, the four genes found in *Z. tritici* were pseudogenes in all sister species due to repeat-induced point mutation (RIP). RIP is a fungal-specific process that is hypothesized to have evolved to stop transposons from proliferating within a genome. RIP is generally recognized by signature C-to-T and G-to-A transitions observed in repetitive sequences (Selker, 2002). Using a consensus alignment approach, the REP9-4 sequences from each of the sister species were de-RIPed so the full gene could be translated and used for phylogenetic analysis. In total we identified 32 sequences with significant similarity to the REP9-4 RVE domain (integrase catalytic core sequence); these included transposases from the Copia (Class I), Polinton (Class II), and IS3EU (Class II) transposon

**TABLE 1** The 28 overlapping differentially expressed genes in comparisons of WAI321 with WAI323 and WAI332, and EffectorP (v1 and v2) predictions (sorted by gene ID)

Name	Description	Length (amino acids)	No. of cysteines	No. of BLAST hits	Probability (EffectorP_v1)	Probability (EffectorP_v2)
Down-regulated in WAI321						
Chr01.828 (REP9-1, 9 copies)	Unnamed protein product	193	6	3	.947	.578
Chr01.876	Unnamed protein product	195	0	10	.978	.619
Chr03.1269	Zn2-Cys6 binuclear cluster domain containing protein	181	4	10	.933	.812
Chr04.792	Hypothetical protein T139_contig4365g00001	89	9	1	1	.952
Chr08.156	Amino acid permease inda1	182	0	10	.738	.731
Chr08.203	-NA-	75	3	0	.999	.903
Chr08.204	-NA-	100	3	0	.987	.619
Chr08.371	Unnamed protein product	159	0	10	.943	.665
Chr08.847	-NA-	57	6	0	1	.841
Chr09.342	-NA-	183	3	0	.901	.797
Chr09.385	Hypothetical protein MYCGRDRAFT_95759	207	3	7	.976	.758
Chr10.642	Glutathione-dependent formaldehyde activating family	259	10	10	.739	.601
Chr10.705	C6 transcription factor	148	6	10	.995	.582
Chr11.12	Unnamed protein product	198	0	10	.976	.670
Chr11.455	Hit family 1	135	2	10	.970	.697
Chr13.76	-NA-	127	4	0	.974	.602
Up-regulated in WAI321						
Chr01.1049	Unnamed protein product	89	6	1	.986	.747
Chr02.843	Unnamed protein product	214	2	10	.691	.868
Chr06.411	HSP20-like chaperone	235	1	10	.572	.551
Chr10.494	-NA-	83	9	0	1	.959

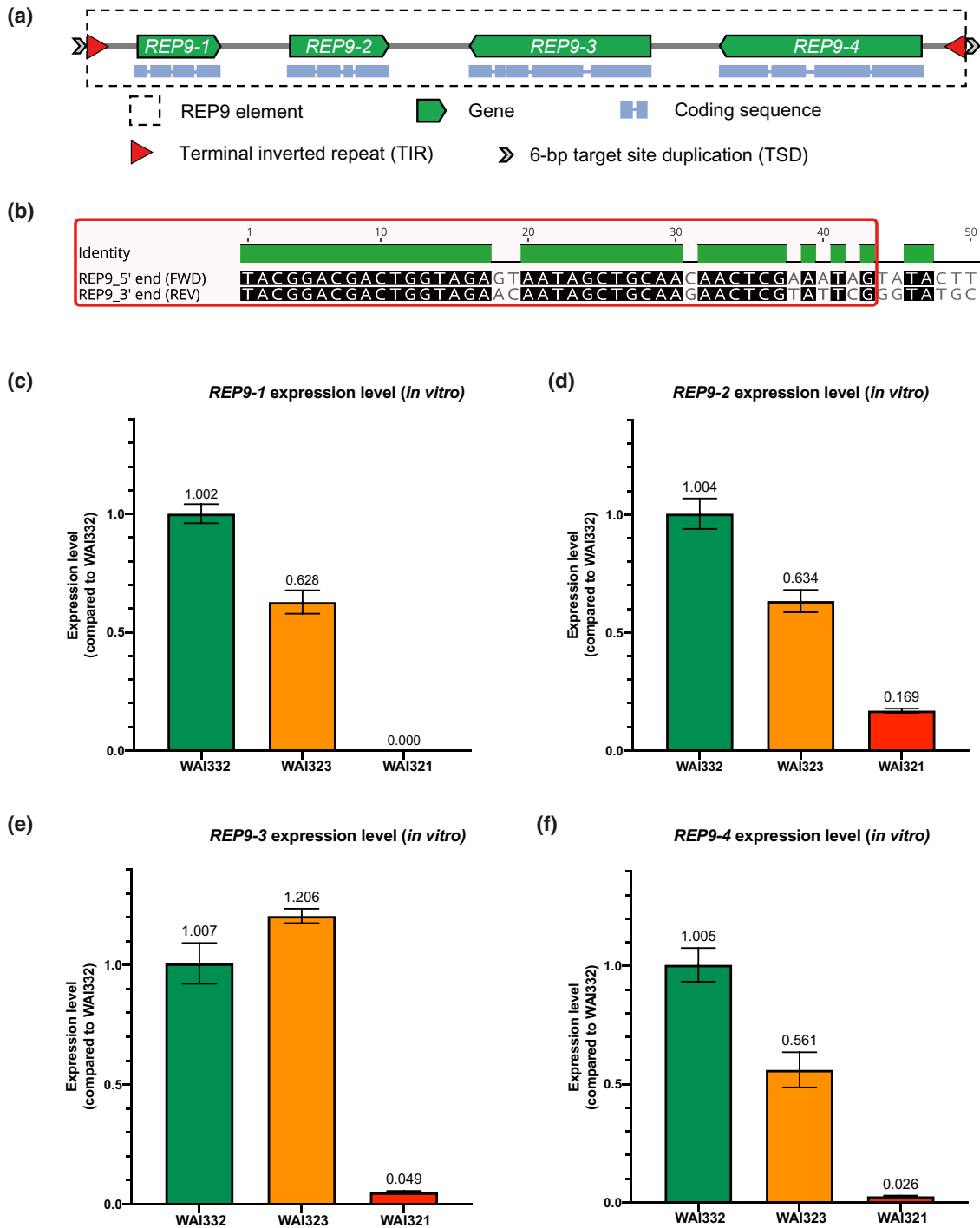


**FIGURE 3** The REP9 element in *Zymoseptoria tritici*. (a) Schematic drawing showing the genes, coding sequences, terminal inverted repeats (TIRs), and target site duplication (TSD) of the REP9 element. REP9 is 7.9 kb in size and consists of four genes, REP9-1, REP9-2, REP9-3, and REP9-4. (b) The alignment of the 5' and 3' ends of the REP9 element showing the 43-bp TIRs. (c, d, e, f) In vitro expression levels of REP9-1, REP9-2, REP9-3, and REP9-4 in the three wild-type *Z. tritici* strains. Bars indicate  $\pm$ SEM

superfamilies (Figure S2). To investigate the evolutionary relationships between REP9-4 and the transposase superfamilies listed above, we constructed a maximum-likelihood (ML) phylogenetic tree (Figure 4). This tree indicates that the integrase domain from REP9-4 is most closely related to transposases found within the IS3EU transposon superfamily, a poorly characterized superfamily

that has only been published in the transposon database RepBase (Bao et al., 2015; Kojima, 2019).

To determine the existence and the copy number of REP9 in isolates WAI321 and WAI323, these genomes were de novo assembled using long-read data. Local BLASTn results suggested that the genome sequence of the high-virulence isolate WAI321 contains 11 copies,



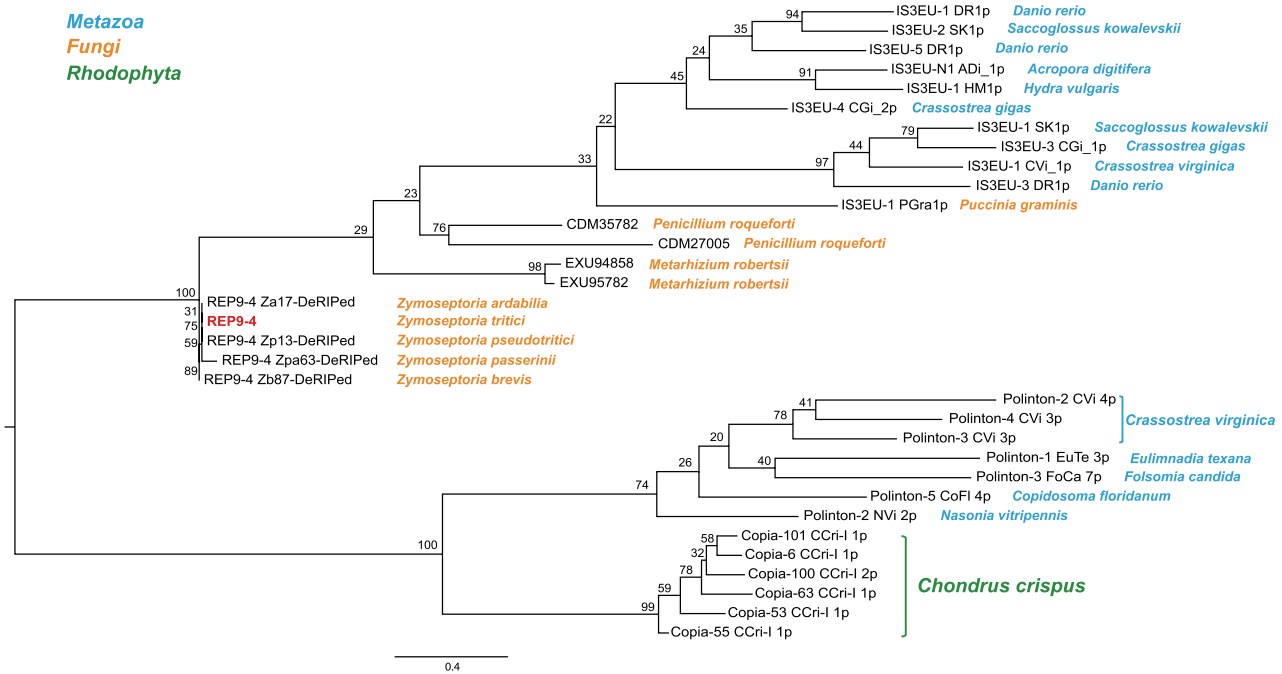


**FIGURE 4** Phylogenetic analysis of REP9-4. Maximum-likelihood (ML) phylogenetic tree of the conserved RVE domain. Numbers next to each branch represent bootstrap support values (%) from 1,000 bootstrap replicates. The scale bar at the bottom is distance in substitutions/site. Species names are listed next to either the NCBI accession number or the transposon name in RepBase. These names are coloured according to the legend located at the top left

while the genome sequence of the medium-virulence isolate WAI323 contains 16 copies of REP9 (Figure S3a). This indicated that this transposon may still be active within *Z. tritici*. In total, we identified 36 REP9 copies in the three long-read assemblies generated for this study. Of those 36 copies, 33 showed 6-bp target site duplications (TSDs) at their integration sites (Figure S3a,b), another feature of Class II transposons (Wicker et al., 2007). Aside from the conserved size, 6 bp, there was no clear consensus sequence for the TSDs (Figure S3b).

## 2.5 | REP9-1 copy number is not correlated with gene expression

The de novo assemblies of all three isolates provided the opportunity to examine whether REP9 copy number could be correlated with REP9-1 gene expression. Sequence conservation of REP9 (7.9 kb) was highest in the low-virulence isolate, WAI332. In this isolate, eight of the nine REP9 copies were identical and the final copy contained a 5-bp indel and six single-nucleotide polymorphisms (SNPs). These indels and SNPs only affected the coding sequence (CDS) of the REP9-2 protein. In WAI332, all nine identical REP9-1 copies encode the full-length (193-amino acid) protein. In comparison, the medium-virulence isolate WAI323 possessed 16 unique REP9 copies (Figure S3), eight of which encoded the full-length REP9-1 protein (Figure S4a). Despite having a similar number of gene copies, WAI323 expressed REP9-1 at significantly lower levels compared to WAI332 in vitro. In planta, the expression of WAI323 REP9-1 was also lower than that of WAI332 at 9 dpi but not at 14 dpi. In the high-virulence isolate WAI321 there

were 11 unique REP9 copies (Figure S3), but only two copies encoded a full-length REP9-1 protein (Figure S4b). Despite WAI321 having two full-length copies of the REP9-1 gene, this gene was not expressed at detectable levels during *in vitro* or *in planta* growth (Figures 3c and S1d). We observed two SNPs in the promoter region of these REP9-1 copies (Figure S4c). Notably, the SNPs of the REP9-1 sequences (as well as other SNPs in the REP9 element) in WAI323 and WAI321 were mainly C-to-T and G-to-A mutations, an indication that these regions were affected by RIP (Figure S4e,f). REP9-1 and REP9-4 were differentially expressed in planta between WAI321 and both lower virulence isolates. Homology searches did not uncover a potential function for REP9-1. Therefore, we focused the functional analysis on REP9-1 using both the low-virulence and high-virulence isolates, WAI332 and WAI321, as two independent genetic backgrounds.

## 2.6 | REP9-1 negatively impacts the asexual reproduction of Z. tritici during infection

To investigate the functional role of REP9-1, independent of the other three genes within REP9, we conducted two separate experiments in the genetic backgrounds of WAI332 (low virulence) and WAI321 (high virulence). In the low-virulence isolate WAI332, we sought to reduce the expression of REP9-1 using RNAi. REP9-1-silenced transformants were generated by randomly integrating a 158-bp sequence (antisense to exon 2 of REP9-1) in WAI332. In parallel, we performed a REP9-1 over-expression (OE) experiment in the high-virulence isolate WAI321, in which the REP9-1 gene with its native (NA) promoter from WAI332 was

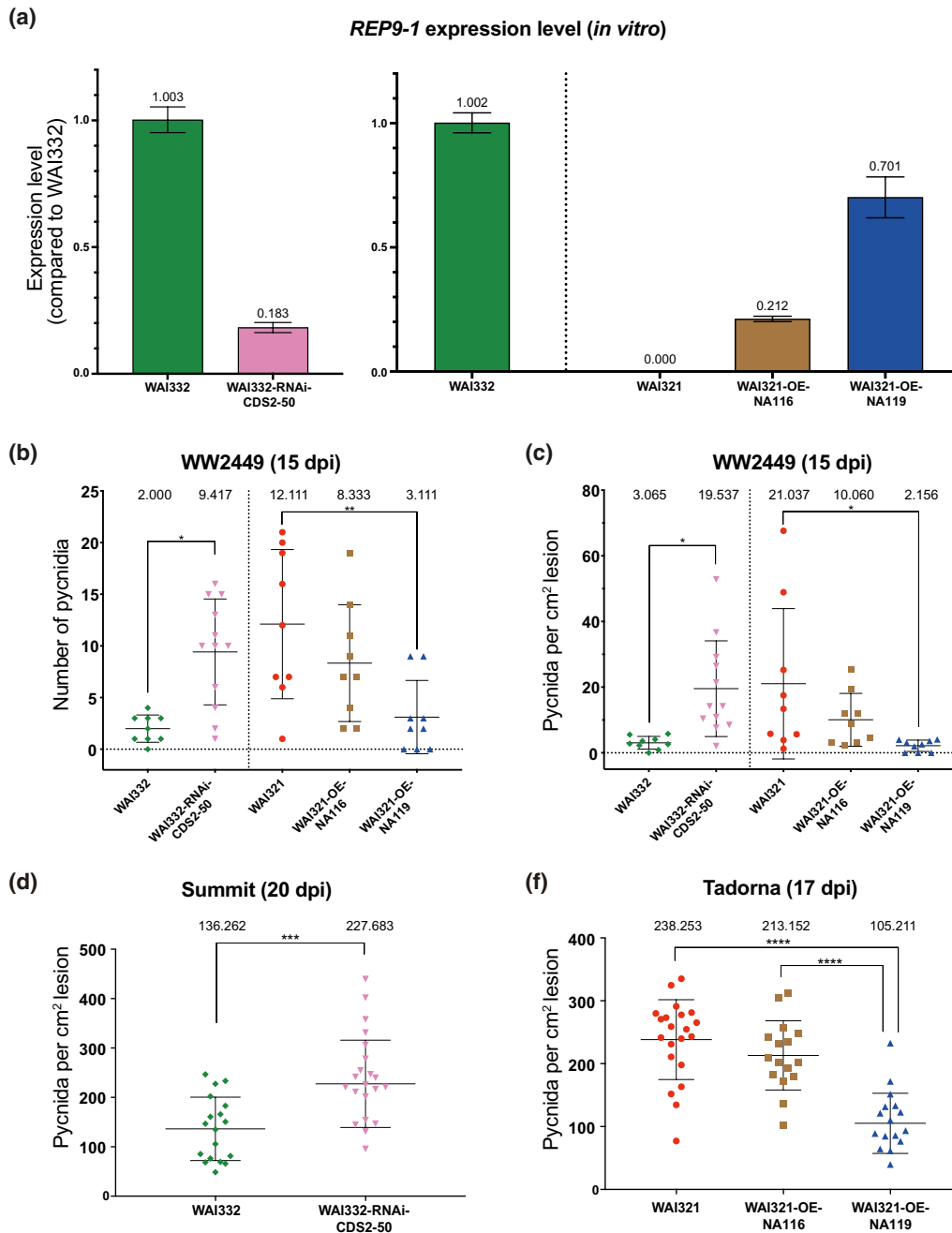


**FIGURE 5** *REP9-1* expression levels in the mutants and the results of the infection assay. (a) The in vitro expression level of *REP9-1* in both RNAi and overexpression (OE) mutants. The *REP9-1* silencing mutant WAI332-RNAi-CDS2-50 in the WAI332 background showed 18.3% expression of *REP9-1* compared to the wild-type (WT) WAI332 (left panel). The two mutants expressing *REP9-1*, WAI321-OE-NA116 and WAI321-OE-NA119, in the WAI321 background showed 21.2% and 70.1% expression of *REP9-1* (compared to the WT WAI332). Bars indicate  $\pm$ SEM. (b) The number of pycnidia produced by WTs and mutants on infected WW2449 leaves. The silencing mutant WAI332-RNAi-CDS2-50 showed an increase in the number of pycnidia produced on the infected leaves compared to the WT WAI332. The two overexpression (OE) mutants WAI321-OE-NA116 and WAI321-OE-NA119 showed a decrease in the number of pycnidia compared to the WT WAI321. Each infection assay was repeated three times and at least nine leaves were collected for each isolate in each experiment. (c) Pycnidia density (pycnidia per  $\text{cm}^2$  lesion) of the WTs and mutants calculated based on the number of pycnidia and the area of necrotic lesions. (d) Pycnidia density produced by the WT WAI332 and the silencing mutant WAI332-RNAi-CDS2-50 on the wheat cultivar Summit at 20 days postinoculation (dpi). Each infection assay was repeated twice and at least 16 leaves were collected for each isolate in each experiment. (e) Pycnidia density produced by WT WAI321 and the two OE mutants WAI321-OE-NA116 and WAI321-OE-NA119 on the wheat cultivar Tadorna. Each infection assay was repeated three times and at least 16 leaves were collected for each isolate in each experiment. All data in (b), (c), (d), and (e) passed the D'Agostino-Pearson normality test (omnibus K2 test); analysis of variance was conducted with the post hoc Tukey multiple comparisons test. Each dot represents an individual leaf sample; numbers on top represent the mean of each group; bars indicate  $\pm$ SD; \* $p < .05$ , \*\* $p < .01$ , \*\*\* $p < .001$ , \*\*\*\* $p < .0001$

knocked into the *sd1* locus. Previous publications show that knock-ins at this locus do not affect the virulence of *Z. tritici* (Kilaru et al., 2015).

For the RNAi silencing construct, we confirmed 33 out of 52 resistant colonies contained the RNAi cassette(s) in their genomes. Fourteen of these 33 mutants were chosen for quantitative PCR (qPCR) analysis and only one mutant (designated WAI332-RNAi-CDS2-50) showed low *REP9-1* expression (18.3%) when compared to the WT WAI332 (Figures 5a and S5a). A mutant WAI332-RNAi-CDS2-10 with 91.0% *REP9-1* expression was included as a transformation control (Figure S5a). For the OE experiment in the WAI321 background, 36 out of 134 resistant colonies were confirmed to have the *REP9-1*-expressing cassette integrated into the *sd1* locus via PCR screening. Eleven of the 36 isolates were subjected to qPCR analysis. Two *REP9-1*-expressing mutants, WAI321-OE-NA116 (21.2% *REP9-1* expression compared to WT WAI332) and WAI321-OE-NA119 (70.1% *REP9-1* expression), were used for subsequent infiltration assays (Figures 5a and S5a). A low-*REP9-1* expression mutant, WAI321-OE-NA79 (10.4%), was also included as a transformation control (Figure S5a). Notably, for the OE mutants, the expression of *REP9-1* induced the expression of the other three genes in the REP9 element *in vitro*; in contrast, the *in vitro* expression of *REP9-2*, *REP9-3*, and *REP9-4* was not affected in the *REP9-1* RNAi-silenced transformants (Figure S5b–d).

First, both the WTs and mutants were tested on the cultivar WW2449. Silencing of *REP9-1* in the low-virulence isolate WAI332 led to a significant increase in the isolate's ability to sporulate on WW2449 (Figure 5b,c). Conversely, OE of *REP9-1* in the high-virulence isolate WAI321 led to a decrease in the mutants' ability to produce pycnidia during infection on WW2449 (Figure 5b,c). The two OE mutants expressed *REP9-1* at different levels, whereby higher expression of *REP9-1* relative to the WT WAI321 was associated with fewer pycnidia (and lower pycnidia density) produced by the mutants on infiltrated leaves (Figure 5b,c). These results suggest that expression of *REP9-1* negatively impacts *in planta* pycnidia production in two distinct genetic backgrounds.

To check whether this change in virulence in the transformants was cultivar-specific, two additional susceptible cultivars (Summit and Millewa) were used to test the RNAi mutant's ability to sporulate in comparison to the WT WAI332. While WAI332 is only weakly pathogenic on WW2449 and Millewa, it is highly pathogenic on the cultivar Summit (McDonald et al., 2016). Consistent with the trend observed on WW2449, the silencing mutant WAI332-RNAi-CDS2-50 showed significantly higher pycnidia density on Summit and Millewa when compared to the WT WAI332 (Figures 5d and S6a). To test this lack of cultivar specificity in the WAI321 (high virulence) background, two additional wheat cultivars (Tadorna and Hereward) highly susceptible to this isolate were tested with the OE mutants and WAI321. Consistent with the results of the RNAi experiment, the OE of *REP9-1* in the high-virulence isolate (WAI321) resulted in reduced pycnidia formation in the mutants during infection on Tadorna and Hereward when compared to the WT WAI321 (Figures 5e and S6b). Notably, the higher the *REP9-1* expression level in the mutant, the lower the pycnidia density on infected leaves (Figure 5e). The

transformation controls showed the same phenotype as their corresponding WTs in the infection assays (Figure S7a–e). These results confirmed that the changes in pycnidia production in response to *REP9-1* expression were not cultivar-specific.

To determine if *REP9-1* has any nonvirulence-related function, the mutants were subjected to *in vitro* growth and stress assays. Results suggested that the *in vitro* growth of the mutants was similar to that of their corresponding WTs in yeast sucrose broth (YSB) medium (Figure 6a) and no differences in growth were observed between the mutants and their respective WT isolates in the stress assays (Figure S8). An *in planta* fungal biomass assay was conducted using these isolates. The RNAi mutant showed similar growth to WT WAI332 during the first 2 weeks of infection on WW2449, yet showed a slight increase in biomass at 17 dpi (Figure 6b). The OE mutants showed reduced biomass during infection compared to the WT WAI321 at 17 dpi (Figure 6b). These results suggest that the phenotypic alterations in the mutants were specific to *in planta* conditions.

Collectively, these data demonstrate that the expression of *REP9-1* negatively affects the virulence of *Z. tritici*, with higher expressing strains producing a lower number of pycnidia per cm<sup>2</sup> lesion on infected leaves.

### 3 | DISCUSSION

Here we describe the discovery of a gene named *REP9-1*, which, when expressed, negatively impacts the number of pycnidia produced during *in planta* infection by the fungal wheat pathogen *Z. tritici*. This gene is located within a 7.9-kb Class II transposon that shows evidence of active transposition and contributes to the virulence of *Z. tritici*. This work demonstrates how expression of a gene within a transposon can affect asexual reproduction of an important wheat pathogen.

#### 3.1 | *REP9-1* resides within a Class II transposon conserved within the *Zymoseptoria* genus

*REP9-1* resides in REP9, an active transposable element (TE) consisting of four genes. The functional roles of the *REP9-2* to *REP9-4* genes in this element were not investigated in this study. However, based on the currently available information, we conclude that *REP9-4* is the transposase/integrase in REP9. Phylogenetic analysis of the integrase domain of *REP9-4* showed that it is most closely related to the DDD/E transposases in the IS3EU DNA transposon superfamily (Kojima, 2019). We identified conserved TIRs and 6-bp TSDs at most locations of REP9 in the three long-read genome assemblies generated for this study, which is also consistent with the IS3EU features. Together, these data support the classification of REP9 as a distant member of the IS3EU transposon superfamily. However, the described IS3EU transposons encode only two proteins, while REP9 consists of four proteins (Kojima, 2019).

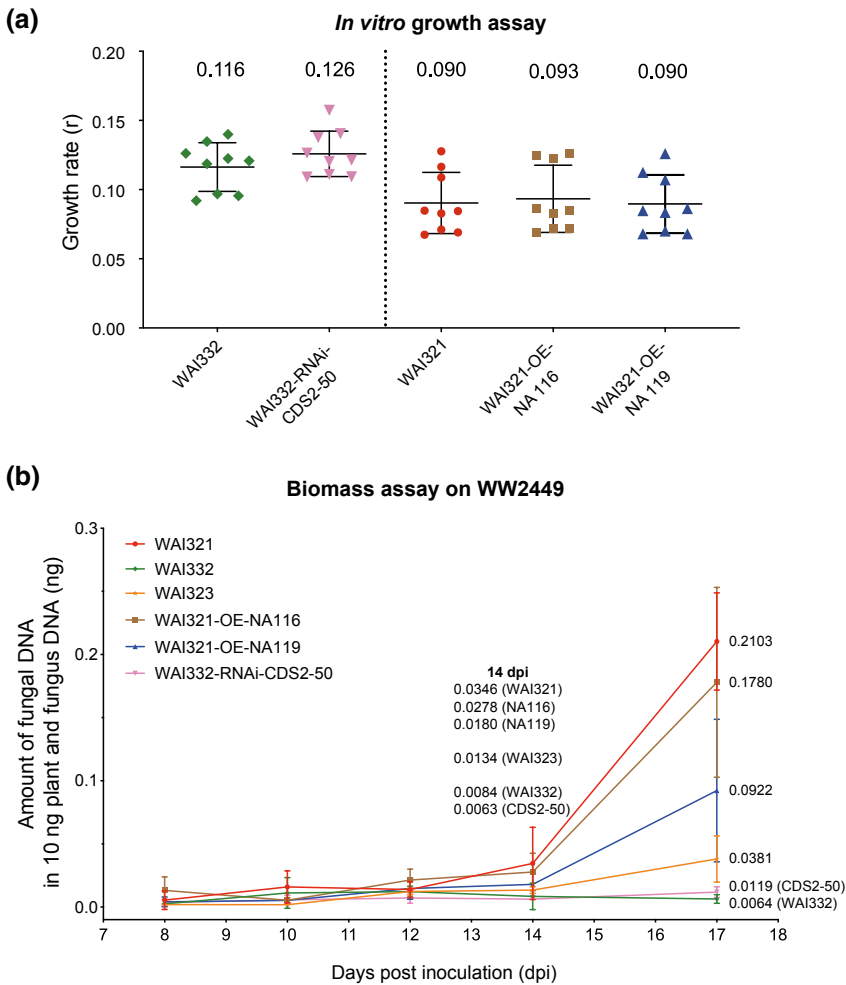


**FIGURE 6** In vitro growth assay and in planta biomass assay for the *Zymoseptoria tritici* wild types (WTs) and mutants. (a) Three independent in vitro growth assays (in yeast sucrose broth medium) were conducted using the *Z. tritici* WT and mutants. The growth rates ( $r$ ) of the mutants were similar to those of their corresponding WT, whereas the two different genetic backgrounds showed significantly different growth rates (Mann–Whitney  $U$  test). Numbers on top represent the mean of each group; bars indicate  $\pm$ SD. (b) Fungal biomass was estimated by quantitative PCR. Values represent the amount of fungal DNA (ng) in 10 ng of total DNA (plant and fungal DNA). The overexpression (OE) mutants showed reduced in planta growth during infection compared to the WT WAI321. Bars indicate  $\pm$ SD

The existence of REP9 (the whole element or fragments) in all currently available long-read sequenced *Z. tritici* and close relatives' genomes indicates that the invasion of this element predates speciation within the *Zymoseptoria* genus (Feurtey et al., 2020). A BLASTn search of the JGI MycoCosm database did not result in any other significant hits, indicating that REP9 may be restricted to the genus. BLASTp of the NCBI nr database did reveal four hits for REP9-1 in four fungal genome assemblies, *Coniochaeta ligniaria* NRRL 30616, *Coniochaeta* sp. 2T2.1, *Fusarium* sp. NRRL 52700, and *Trichoderma gamsii* A5MH. However, all four hits were also found in the REP9-2 BLASTp hit list, indicating that these hits were probably due to the presence of the DUF3716 domain present in both of these proteins. The significant number of BLAST hits for REP9-4 indicate that further long-read assemblies of other close relatives may reveal a wider distribution of the IS3EU transposon superfamily in fungi. Repetitive sequences, especially highly identical multicopy transposons, are often not included in the output contig/scaffolds from short-read de novo assemblers because these reads cannot be uniquely placed in the assembly. This has been clearly shown in *Zymoseptoria* spp., whereby isolates that are resequenced with long-read data have a longer total assembly size compared to assemblies of the same isolate made with short-read data only (Badet et al., 2020; Feurtey et al., 2020). Thus far, we consider

REP9 a novel Class II DNA transposon within the *Zymoseptoria* genus that is most closely related to the IS3EU superfamily.

TEs are thought to contribute to genome evolution through their mobility and tendency to capture nearby DNA or interrupt important coding genes (Bourque et al., 2018). Some TEs, including a few endogenous retroviruses (ERVs), can encode functional proteins that confer direct adverse fitness effects on their host genomes (Bourque et al., 2018). For example, the Env proteins from ERV can be cytotoxic when overexpressed (Perron et al., 2001). While there were no observed toxic effects of *REP9-1* expression in vitro, high *REP9-1* expression significantly reduced an isolate's ability to produce pycnidia in planta. We hypothesize that under field conditions, high *REP9-1* expression could negatively impact the fitness of an isolate by reducing the number of pycnidia, and therefore asexual spores, to splash-disperse up the leaf canopy during the epidemic phase of the disease. This hypothesis is supported by recent experimental evidence from single and mixed infections of *Z. tritici* that showed that an isolate's ability to produce asexual spores during a single infection was a good predictor of how competitive this isolate would be in a mixed infection on the same cultivar (Barrett et al., 2021). The negative fitness effect *REP9-1* expression imposes could be plastic/transient, as transposition of REP9 to a new location within the genome could rapidly alter *REP9-1*

expression in asexual progeny. For the experiments conducted for this work, the expression of *REP9-1* was extremely stable in both the WT and transformation mutants across several independent experiments. However, as discussed above, *REP9* was found in different genomic locations in the three WT isolates, which indicates that active transposition is still occurring in field isolates.

TEs have also been shown to be a rich source of regulatory elements that include transcription factor binding sites and the production of noncoding RNAs (Chuong et al., 2017). The regulatory effects of TEs have been observed in *cis* where the expression of a TE can also influence the expression of nearby genes (Bourque et al., 2018; Chuong et al., 2017). For example, a recent study showed that insertion of TEs directly adjacent to a quantitative avirulence factor, *Avr3D1*, probably reduced the expression of this gene in the high-virulence *Z. tritici* strain 3D7 (Fouché et al., 2019). Notably, in the same study, the authors also observed that TEs and genes with the most similar expression patterns were not near each other in the genome, which suggested that TEs can also modulate gene expression in *trans* (Fouché et al., 2019). In the knock-in experiments conducted here, the *sd1* locus is not near any of the genes that are known to influence pycnidia production; thus, we hypothesize that *REP9-1* could regulate the expression of other genes responsible for pycnidia production in *trans* (Tiley et al., 2019).

### 3.2 | *REP9-1* expression affects the formation of pycnidia in a quantitative manner

Previous work in *Z. tritici* clearly established that necrosis and pycnidia formation were controlled by separate genetic loci (Stewart et al., 2017). While both traits are crucial for facilitating infection, the ability to sporulate on a cultivar greatly facilitates more widespread and severe field epidemics (Parlevliet, 1979; Suffert et al., 2011). The asexual infection cycles of a pathogen are a significant determinant of the total damage it can cause in the field and pycnidiospores are considered the main inoculum source of *Z. tritici* during the STB epidemic period (Parlevliet, 1979; Suffert et al., 2011). During one growing season *Z. tritici* can undergo five or six rounds of asexual reproduction and field experiments have shown that there is selection for more virulent isolates in a single growing season (Karisto et al., 2018; Suffert et al., 2015). Thus, the genes that affect the sporulation ability of *Z. tritici* will have a major impact on the rate and severity of an STB epidemic. In this study, the expression of *REP9-1* showed a negative correlation with pycnidia density on infected leaves. Our results suggest that *REP9-1* has a quantitative role in influencing the virulence of *Z. tritici* regardless of the host genotype.

Thus far only one other gene in *Z. tritici*, *Zt89160*, has been shown to negatively influence pycnidia formation in planta. Specifically, the  $\Delta Zt89160$  strains showed enhanced pycnidia formation during infection, and it was proposed that this gene could play a role in the regulation of virulence-related genes (Poppe et al., 2015). However, unlike *REP9-1*, *Zt89160* has a conserved regulator of chromosome condensation 1 domain, which in other organisms has been linked to a number of nuclear processes (Poppe et al., 2015). *REP9-1* has a domain of unknown

function (DUF3716) and no signal peptide, which makes speculation about its putative function extremely difficult. While *REP9-1* was identified as a potential effector candidate, this is probably a false positive as EffectorP is intended for predicted proteins with signal peptides (Sperschneider et al., 2018). Alterations of *REP9-1* expression did not lead to any visible morphological change of *Z. tritici* under in vitro conditions, which is similar to *Zt89160* and other virulence-related genes (Meile et al., 2018; Poppe et al., 2015). In addition, the in vitro growth rate of the mutants was unaffected compared to their corresponding WTs. Yet, for the genetically modified WAI321 strains, *REP9-1* OE resulted in reduced in planta growth during infection on WW2449, which indicates that the impact of *REP9-1* is specific to in planta conditions. Further functional work is required to dissect whether *REP9-1* regulates pycnidia development through direct interaction with the regulatory proteins/promoters of pycnidiation genes or alternatively through RNA-based regulatory pathways. Additional mechanistic work with a green fluorescent protein (GFP)-expressing strain could also further our understanding of how *REP9-1* influences pycnidia formation in planta. For example, does *REP9-1* expression simply slow the overall growth of the fungus in planta, leading to a delay in pycnidia development? Or does the expression of *REP9-1* actually lead to abnormal or arrested pycnidia development inside the leaf?

It has been previously proposed that three major factors affect the pycnidia production of *Z. tritici* on infected wheat leaves: nutrients, the fitness of the pathogen, and host responses (Stewart & McDonald, 2014), of which the latter two are not mutually exclusive. In our study, the available nutrients should not be the limiting factor for pycnidia formation as all *Z. tritici* strains (WTs and mutants) used were able to cause necrosis on WW2449 leaves. As discussed above, *REP9-1* may have an impact on the in planta development/growth of *Z. tritici* and/or it may be recognized by wheat via yet unknown mechanisms, leading to a quantitative resistance response against the pathogen. Interestingly, many of the coding regions of *REP9* in *Z. tritici* and its close relatives showed clear evidence of RIP. In the sister species there were no remaining active copies of the *REP9* transposon. This could be an indication that *REP9* is under negative selection within *Zymoseptoria* spp. This fits with the hypothesis that genes that have a negative effect on the number of offspring produced, observed here as reduced pycnidia number, would be selected against in large populations.

In conclusion, here we report the first discovery of a multicopy gene, *REP9-1*, that resides in a TE, *REP9*. The *REP9-1* gene negatively regulates the rate of pycnidia appearance in planta of the wheat pathogen *Z. tritici*, adding further complexity to genetic loci that contribute to the virulence of this important pathogen.

## 4 | EXPERIMENTAL PROCEDURES

### 4.1 | *Z. tritici* strains and fungal genome sequencing, assembly, and annotation

The three Australian *Z. tritici* isolates WAI321, WAI323, and WAI332 were collected in wheat fields in Victoria (2012), Tasmania

(2011), and New South Wales (1979), respectively (McDonald et al., 2016). For long-term storage, fungal isolates were maintained in 30% glycerol at  $-80^{\circ}\text{C}$ . *Z. tritici* cultures were grown on yeast sucrose agar (YSA; 10 g/L yeast extract, 10 g/L sucrose, 1.5% agar) at  $20^{\circ}\text{C}$  under a 12/12-hr light/dark cycle for 3 days. Blastospores were scraped from the surface of agar plates and genomic DNA (gDNA) was extracted according to the methods described in McDonald, Taranto, et al. (2019) and on protocols.io (<http://dx.doi.org/10.17504/protocols.io.k6qcqzdw>). For isolate WAI332, two independent 15–20-kb genomic P6 SMRT cell libraries were made at the Ramaciotti Centre for Genomics (UNSW Sydney, Australia). These libraries were sequenced on 13 SMRT cells using the P6-C4 chemistry on a Pacbio RSII instrument (Pacific Biosciences). The genome was assembled de novo using Canu v. 1.5 with “minReadLength = 2000” and “genomeSize” set to 41 Mb (Koren et al., 2017). Assembled contigs were further corrected using the SMRT Analysis package v. 2.3.0. First the raw Pacbio reads were mapped to the *de novo* assembly with blaser with the following settings: --seed = 1, --minAccuracy = 0.75, --minLength = 500, --forQuiver, --algorithmOptions = '-minMatch 12 -bestn 1 -minPctIdentity 65.0', --hitPolicy = randombest (Chaisson & Tesler, 2012). The resulting bam file was used as input for Quiver to call a new consensus sequence with the following settings: makeVcf = True, makeBed = True, enableMapQVFilter = T, minConfidence = 40, minCoverage = 10, diploidMode = False (Vaser et al., 2017). For isolates WAI321 and WAI323, gDNA was extracted as above. DNA sequencing libraries were constructed with Oxford Nanopore's 1D SQK-LSK108 kit and sequenced on R9.4.1 flow cells. Raw nanopore reads were base-called using Albacore v. 2.1.3. Base-called reads were assembled in Canu v. 1.6 with “minReadLength = 3,000” and “genomeSize = 40 Mb.” Assemblies were polished with Nanopolish v. 0.9.0 (Loman et al., 2015) followed by short-read correction with Pilon v. 1.22 (Walker et al., 2014). Previous in vitro Illumina RNA-Seq data generated in our laboratory were used for gene prediction via CodingQuarry v. 2.0 (Testa et al., 2015). The genome of WAI332 has 15,059 predicted gene models. A list of the three assemblies and basic genome quality statistics are provided in Table S5. The contigs in these three genome assemblies were named based on synteny alignments to the reference isolate IPO323 assembly.

#### 4.2 | Plant infection and RNA-sequencing

*Z. tritici* blastospores were collected as described above, counted in a haemocytometer, and diluted to a concentration of  $10^6$  spores/ml in 0.02% Tween 20. This suspension was sprayed onto the third leaves of 3-week-old wheat seedlings (cultivar WW2449). The inoculated plants were kept in the dark at high humidity for 48 hr inside sealed black plastic boxes at  $22^{\circ}\text{C}$ . After this incubation period, the plants were kept in a controlled environment chamber with a 16/8-hr day/night cycle ( $20^{\circ}\text{C}$  day and  $12^{\circ}\text{C}$  night). The infected leaf samples and a Tween 20-only negative control were collected at

9 and 14 dpi. Each biological replicate was composed of four leaves from four different infected plants. In total, four biological replicates were collected for each treatment at both time points. Harvested leaves were frozen immediately after being cut from the plant in liquid nitrogen and all samples were stored at  $-80^{\circ}\text{C}$  until RNA extraction. Total RNA was extracted with the Quick-RNA Fungal/Bacterial Miniprep Kit (R2014; Zymo Research) with an on-column DNase treatment (DNASE70-1SET; Sigma-Aldrich). The extracted RNA was checked by gel electrophoresis and quantified with both a NanoDrop ND-1000 (Thermo Fisher Scientific) and a Qubit 2.0 Fluorometer (Invitrogen). High-quality RNA was submitted for sequencing at the Ramaciotti Centre for Genomics (UNSW, Sydney, Australia). Here, libraries were generated using the Illumina TruSeq Stranded mRNA-Seq kit. Three libraries were pooled per NextSeq500 75-bp SR run. In total, 30 mRNA libraries were sequenced across 10 NextSeq500 runs. Samples were randomly distributed across sequencing runs, ensuring that individual isolates were never sequenced together with their biological replicate from either time point.

#### 4.3 | Transcriptome mapping and differential gene expression analysis

Trimmomatic v. 0.33 (Bolger et al., 2014) was used to remove adapters and trim low-quality bases in the raw Illumina reads with -phred33 ILLUMINACLIP: TruSeq3-SE.fa:2:30:10 LEADING:10 TRAILING:10 SLIDINGWINDOW:4:15 MINLEN:50. FASTQC was used before and after trimming for quality control. The splice-aware aligner STAR v. 2.5.3 (Dobin et al., 2013) was used to align the filtered reads to the WAI332 reference genome. The default settings of STAR were used except for minimum and maximum intron sizes (-alignIntronMin10; -alignIntronMax1000). Mapped reads that overlapped with annotated transcripts were quantified using Stringtie v. 1.3.3 (--rf -e -B -G) and the corresponding read counts information was extracted by the Python script (prepDE.py) provided by Stringtie (Pertea et al., 2015). The edgeR (Robinson et al., 2010) package in R was then used for the DEG analysis. Read counts for each transcript were normalized using the TMM method implemented in the edgeR package and three sets of DEGs were identified between each two of the three isolates. One sample (WAI321\_14dpi\_rep4) was discarded as it did not group appropriately with the other replicates. Top DEGs were subjected to analyses using NCBI, EffectorP (Sperschneider et al., 2016, 2018), and PHYRE2 (Kelley et al., 2015). The DEG clustering analysis was performed using pheatmap (Kolde, 2015) in R.

#### 4.4 | Phylogenetic relationships

A BLASTp database was generated using all the transposon sequences (as of 2020-09-25) on RepBase (Bao et al., 2015) and the REP9-4 protein sequence was used as the query in a BLAST search against the database. Sequences (coverage) longer than 90 amino acids with a pairwise identity of over 20% with REP9-4 were

selected for the sequence alignment. The four functionally annotated BLASTp hits from NCBI and the REP9-4 (De-RIPed version) from the other *Zymoseptoria* species were also included in the alignment. For the de-RIPing of REP9-4 proteins, we first extracted the REP9-4 sequences with the highest pairwise identity with *Z. tritici* REP9-4 from the other *Zymoseptoria* species and manually changed the G-to-A and C-to-T SNPs. The de-RIPed sequences were then translated into protein sequences.

InterProScan (Quevillon et al., 2005) was used to identify the conserved domain(s) in the BLAST hits. The sequences around the conserved RVE domain region were extracted and aligned with Muscle v. 3.8.425 (Edgar, 2004). The final trimmed alignment length was 205 amino acids. This alignment was used to construct an ML phylogenetic tree. RaxML v. 8.2.11 (Stamatakis, 2014) was used to find the highest-scoring ML tree using the “-f a -x 1” algorithm (rapid bootstrap analysis and searching for the best ML tree), the general time reversible AA substitution (GTR) model with a gamma distribution to account for variation in mutation rates at different sites and 1,000 bootstrap replicates. The random seed used for this search was 3.

#### 4.5 | Generation of RNAi and REP9-1 expression constructs

All primers used in this study are listed in Table S6. To generate the plasmid for targeted gene integration, two flanking regions (c.1 kb in size) for homologous recombination were amplified from *Z. tritici* WAI332 gDNA with primers 5flk\_F\_ovh, 5flk\_R, 3flk\_F\_Hyg\_ovh, and 3flk\_R\_ovh. The primers amplify the *sdi1* locus described by Kilaru et al. (2015) between the *Mycgr3G74146* and *Mycgr3G45644* genes in IPO323 (Goodwin et al., 2011). The hygromycin resistance gene (*Hyg*), used as a selectable marker, was amplified from pGpD-eGFP (Sexton & Howlett, 2001) using primers PtpC-Hyg-5-F and PtpC-Hyg-3-R. The REP9-1 sequence with promoter and overhangs was amplified from WAI332 gDNA using primers R9-1\_5ovh\_F and R9-1\_Hyg\_3ovh\_R. The four fragments were assembled into the vector plasmid and extracted as previously described (Khan et al., 2020) using the yeast (*Saccharomyces cerevisiae*) homologous recombination system (Raymond et al., 1999). The extracted plasmids were transformed into *Escherichia coli* and screened by colony PCR (for the *Hyg* fragment) and restriction analysis (*Sma*I digestion). The resulting plasmid was transformed into WAI321 via *Agrobacterium tumefaciens*-mediated transformation according to Protocol Exchange (2008) (<https://doi.org/10.1038/nprot.2008.83>). Gene insertion into the correct locus was confirmed by PCR using primers HY-primer-F and R9-1\_Insertion-check\_3R.

An antisense CDS of REP9-1 (158-bp REP9-1 CDS2 reverse complement sequence) with overhangs was amplified from cDNA using primers R9-1\_CDS2rc-ovh-F and R9-1\_CDS2rc-ovh-R. This fragment was introduced into the vector pBARGPE1-LIC via Gibson assembly (New England Biolabs) according to Lin et al. (2018). The assembled

RNAi plasmid was checked by sequencing using primers pBAR\_insert\_Check\_F and pBAR\_insert\_Check\_R. The resulting plasmid was transformed into WAI332 via polyethylene glycol-mediated protoplast transformation, as previously described (Solomon et al., 2003). The transformants were selected on minimal medium (with ammonium tartrate as the only nitrogen source) containing 2 µl/ml phase-extracted glufosinate ammonium aqueous. Gene insertion was confirmed by PCR using primers GPE1-F and TtrpC-seq-R. Takara ExTaq was used for all PCRs.

#### 4.6 | RNA isolation and real-time quantitative PCR

For each sample,  $10^7$  *Z. tritici* spores were inoculated in 50 ml YSB and grown for 60 hr at 20 °C under shaking at 140 rpm. *Z. tritici* cultures were harvested by centrifugation for 5 min at  $3,724 \times g$ . After centrifugation the supernatant was discarded and the samples were immediately frozen in liquid nitrogen and stored at -80 °C. Total RNA was isolated using the Quick-RNA Fungal/Bacterial extraction kit (Zymo Research). Possible DNA contamination was removed using the TURBO DNA-free Kit (Thermo Fisher Scientific). cDNA was synthesized from 0.2 µg RNA using the SuperScript IV First-Strand Synthesis System (Thermo Fisher Scientific). qPCR was performed as previously described (Lin et al., 2018) using primers R9-1\_qpcr\_F, R9-1\_qpcr\_R, R9-2\_qpcr\_F, R9-2\_qpcr\_R, R9-3\_qpcr\_F, R9-3\_qpcr\_R, R9-4\_qpcr\_F, R9-4\_qpcr\_R, Actin\_qpcr\_F, and Actin\_qpcr\_R. The expression of REP9-1 in WT WAI332 was set as 1. Relative expression of REP9-1 to REP9-4 was calculated by normalizing against the expression of *Actin* (endogenous control).

#### 4.7 | Pathogenicity assays and quantification of disease

*Z. tritici* isolates were grown for 4 days on YSA as described above. Blastospores were counted in a haemocytometer and diluted to a concentration of  $10^6$  spores/ml. Pathogenicity was assessed by infiltrating spore suspensions into the third leaves of 3-week-old wheat seedlings as described previously (Yang et al., 2018). The inoculated plants were then kept in controlled environment chambers with the same conditions as described above. To measure the total necrotic area and count the number of pycnidia per lesion (pycnidia density), the cut leaves were mounted on paper sheets, scanned with a flatbed scanner at 1,200 dots per inch (EPSON), and analysed using automated image analysis (Karisto et al., 2018). Leaves were generally harvested 3–5 days after pycnidia first appeared depending on the disease development and senescence on a given cultivar. Due to senescence seen on WW2449 leaves after 17 dpi, infiltrated leaves were assessed at 15 to 17 dpi. Differences in pycnidia number and pycnidia density were tested using one-way analysis of variance with the post hoc Tukey honestly significant difference test for comparing multiple treatments.

## 4.8 | In planta biomass assay and in vitro growth assay

The fungal biomass (amount of fungal DNA) in infected WW2449 leaves was measured by qPCR according to Zhong et al. (2017), with a few minor adjustments. *Z. tritici* spore suspensions were infiltrated into wheat cultivar WW2449 and the regions around the watermarks were marked for cutting. In this assay, newly grown leaves were cut to keep the infiltrated leaves green during the course of collection (i.e., before disease symptoms were visible). The infiltrated leaves (four replicate leaves for each strain, around 4 cm in length) were collected at 8, 10, 12, 14, and 17 dpi and subjected to gDNA extraction by the QIAGEN plant DNA extraction kit. The gDNA concentration of all samples was adjusted to 10 ng/μl and gDNA was used for qPCR with primers Zt-TRP-qpcr-F and Zt-TRP-qpcr-R. The qPCR data were analysed via the standard curve method using QuantStudio software.

The in vitro growth assay was adapted from Möller et al. (2018). Briefly,  $10^7$  *Z. tritici* spores were inoculated in 50 ml YSB and grown for 6 days under shaking at 140 rpm at 20 °C under a 12/12-hr day/night cycle. Each sample was grown in biological triplicate. Growth was analysed by measuring the optical density at 600 nm; samples were diluted 1:5, 1:10, or 1:20 depending on the concentration to obtain accurate measurements. The R package Growthcurver was used to model growth curves for each isolate (Sprouffske & Wagner, 2016). The Mann–Whitney *U* test was used to test for significant differences in growth rates (*r*) between strains.

## 4.9 | Stress and development assay

To test if there were any differences in growth under stress, blastospores from 3-day-old cultures of both WTs WAI332 and WAI321 and all mutants (3 μl of  $10^6$  spores/ml and three 1:10 serial dilutions) were inoculated on YSA plates and YSA supplemented with H<sub>2</sub>O<sub>2</sub> (2 and 4 mM), NaCl (0.5 and 1 M), or sorbitol (1 and 1.5 M) and incubated for 6 days at 20 °C.

### ACKNOWLEDGEMENTS

All authors wish to acknowledge the plant service team at the Australian Plant Phenomics Facility, which is supported under the National Collaborative Research Infrastructure Strategy of the Australian Government. C.W. acknowledges the support of the Australian National University–China Scholarship Council joint scholarship. M.C.M. is supported by the Australian National University, Grains and Research Development Corporation and NSW Department of Primary Industries co-investment DAN00203 as part of the Grains, Agronomy and Pathology Partnership. We also thank two anonymous reviewers whose comments have significantly improved this manuscript.

### DATA AVAILABILITY STATEMENT

All raw RNA-Seq and genome sequencing data and associated assemblies are deposited under NCBI project PRJNA604047.

CodingQuarry gene predictions for isolate WAI332, REP9-4 RVE protein alignment, and the PHYRE2 structural predictions are provided on GitHub ([https://github.com/SolomonLab/REP9-1\\_Supplementary\\_Info](https://github.com/SolomonLab/REP9-1_Supplementary_Info)).

### ORCID

Chen Wang  <https://orcid.org/0000-0002-0508-0084>

Andrew W. Milgate  <https://orcid.org/0000-0001-6237-9018>

Peter S. Solomon  <https://orcid.org/0000-0002-5130-7307>

Megan C. McDonald  <https://orcid.org/0000-0002-9129-7393>

### REFERENCES

- Agrios, G. (2005) *Plant Pathology*. Burlington, MA, USA: Elsevier Academic Press.
- Badet, T., Oggenfuss, U., Abraham, L., McDonald, B.A. & Croll, D. (2020) A 19-isolate reference-quality global pangenome for the fungal wheat pathogen *Zymoseptoria tritici*. *BMC Biology*, 18, 12.
- Bao, W., Kojima, K.K. & Kohany, O. (2015) Repbase Update, a database of repetitive elements in eukaryotic genomes. *Mobile DNA*, 6, 1–6.
- Barrett, L.G., Zala, M., Mikaberidze, A., Alassimone, J., Ahmad, M., McDonald, B.A. et al. (2021) Mixed infections alter transmission potential in a fungal plant pathogen. *Environmental Microbiology*. <https://doi.org/10.1111/1462-2920.15417>
- Bolger, A.M., Lohse, M. & Usadel, B. (2014) Trimmomatic: a flexible trimmer for Illumina sequence data. *Bioinformatics*, 30, 2114–2120.
- Bos, L. & Parlevliet, J.E. (1995) Concepts and terminology on plant/pest relationships: toward consensus in plant pathology and crop protection. *Annual Review of Phytopathology*, 33, 69–102.
- Bourque, G., Burns, K.H., Gehring, M., Gorbunova, V., Seluanov, A., Hammell, M. et al. (2018) Ten things you should know about transposable elements. *Genome Biology*, 19, 199.
- Brown, J.K.M., Chartrain, L., Lasserre-Zuber, P. & Sainetac, C. (2015) Genetics of resistance to *Zymoseptoria tritici* and applications to wheat breeding. *Fungal Genetics and Biology*, 79, 33–41.
- Brunner, P.C., Stefanato, F.L. & McDonald, B.A. (2008) Evolution of the *CYP51* gene in *Mycosphaerella graminicola*: evidence for intragenic recombination and selective replacement. *Molecular Plant Pathology*, 9, 305–316.
- Chaisson, M.J. & Tesler, G. (2012) Mapping single molecule sequencing reads using basic local alignment with successive refinement (BLASR): application and theory. *BMC Bioinformatics*, 13, 238.
- Chuong, E.B., Elde, N.C. & Feschotte, C. (2017) Regulatory activities of transposable elements: from conflicts to benefits. *Nature Reviews Genetics*, 18, 71–86.
- Dobin, A., Davis, C.A., Schlesinger, F., Drenkow, J., Zaleski, C., Jha, S. et al. (2013) STAR: ultrafast universal RNA-seq aligner. *Bioinformatics*, 29, 15–21.
- Edgar, R.C. (2004) MUSCLE: Multiple sequence alignment with high accuracy and high throughput. *Nucleic Acids Research*, 32, 1792–1797.
- Estep, L.K., Torriani, S.F.F., Zala, M., Anderson, N.P., Flowers, M.D., McDonald, B.A. et al. (2015) Emergence and early evolution of fungicide resistance in North American populations of *Zymoseptoria tritici*. *Plant Pathology*, 64, 961–971.
- Fourtey, A., Lorrain, C., Croll, D., Eschenbrenner, C., Freitag, M., Habig, M. et al. (2020) Genome compartmentalization predates species divergence in the plant pathogen genus *Zymoseptoria*. *BMC Genomics*, 21, 588.
- Fones, H. & Gurr, S. (2015) The impact of *Septoria tritici* blotch disease on wheat: an EU perspective. *Fungal Genetics and Biology*, 79, 3–7.
- Fouché, S., Badet, T., Oggenfuss, U., Plissonneau, C., Francisco, C.S. & Croll, D. (2019) Stress-driven transposable element de-repression dynamics and virulence evolution in a fungal pathogen. *Molecular Biology and Evolution*, 37, 221–239.



- Goodwin, S.B., Ben M'Barek, S., Dhillon, B., Wittenberg, A.H.J., Crane, C.F., Hane, J.K. et al. (2011) Finished genome of the fungal wheat pathogen *Mycosphaerella graminicola* reveals dispensome structure, chromosome plasticity, and stealth pathogenesis. *PLoS Genetics*, 7, e1002070.
- Haueisen, J., Möller, M., Eschenbrenner, C.J., Grandaubert, J., Seybold, H., Adamiak, H. et al. (2019) Highly flexible infection programs in a specialized wheat pathogen. *Ecology and Evolution*, 9, 275–294.
- Karisto, P., Hund, A., Yu, K., Anderegg, J., Walter, A., Mascher, F. et al. (2018) Ranking quantitative resistance to *Septoria tritici* blotch in elite wheat cultivars using automated image analysis. *Phytopathology*, 108, 568–581.
- Kelley, L.A., Mezulis, S., Yates, C.M., Wass, M.N. & Sternberg, M.J.E. (2015) The Phyre2 web portal for protein modeling, prediction and analysis. *Nature Protocols*, 10, 845–858.
- Kellner, R., Bhattacharyya, A., Poppe, S., Hsu, T.Y., Brem, R.B. & Stukenbrock, E.H. (2014) Expression profiling of the wheat pathogen *Zymoseptoria tritici* reveals genomic patterns of transcription and host-specific regulatory programs. *Genome Biology and Evolution*, 6, 1353–1365.
- Kema, G.H.J., Mirzadi Gohari, A., Aouini, L., Gibriel, H.A.Y., Ware, S.B., van den Bosch, F. et al. (2018) Stress and sexual reproduction affect the dynamics of the wheat pathogen effector AvrStb6 and strobilurin resistance. *Nature Genetics*, 50, 375–380.
- Keon, J., Antoniw, J., Carzaniga, R., Deller, S., Ward, J.L., Baker, J.M. et al. (2007) Transcriptional adaptation of *Mycosphaerella graminicola* to programmed cell death (PCD) of its susceptible wheat host. *Molecular Plant-Microbe Interactions*, 20, 178–193.
- Keon, J., Rudd, J.J., Antoniw, J., Skinner, W., Hargreaves, J. & Hammond-Kosack, K. (2005) Metabolic and stress adaptation by *Mycosphaerella graminicola* during sporulation in its host revealed through microarray transcription profiling. *Molecular Plant Pathology*, 6, 527–540.
- Khan, H., McDonald, M.C., Williams, S.J. & Solomon, P. (2020) Assessing the efficacy of CRISPR/Cas9 genome editing in the wheat pathogen *Parastagonospora nodorum*. *Fungal Biology and Biotechnology*, 7, 4.
- Kilaru, S., Schuster, M., Latz, M., Das Gupta, S., Steinberg, N., Fones, H. et al. (2015) A gene locus for targeted ectopic gene integration in *Zymoseptoria tritici*. *Fungal Genetics and Biology*, 79, 118–124.
- Kojima, K.K. (2019) Structural and sequence diversity of eukaryotic transposable elements. *Genes & Genetic Systems*, 94, 233–252.
- Kolde, R. (2015) pheatmap: pretty heatmaps. *R Package. version 1.0.8*, 1–7.
- Koren, S., Walenz, B.P., Berlin, K., Miller, J.R., Bergman, N.H. & Phillippy, A.M. (2017) Canu: Scalable and accurate long-read assembly via adaptive  $\kappa$ -mer weighting and repeat separation. *Genome Research*, 27, 722–736.
- Lee, W.-S., Rudd, J.J., Hammond-Kosack, K.E. & Kanyuka, K. (2014) *Mycosphaerella graminicola* LysM effector-mediated stealth pathogenesis subverts recognition through both CERK1 and CEBiP homologues in wheat. *Molecular Plant-Microbe Interactions*, 27, 236–243.
- Lin, S.Y., Chooi, Y.H. & Solomon, P.S. (2018) The global regulator of pathogenesis PnCon7 positively regulates *Tox3* effector gene expression through direct interaction in the wheat pathogen *Parastagonospora nodorum*. *Molecular Microbiology*, 109, 78–90.
- Loman, N.J., Quick, J. & Simpson, J.T. (2015) A complete bacterial genome assembled de novo using only Nanopore sequencing data. *Nature Methods*, 12, 733–735.
- Marshall, R., Kombrink, A., Motteram, J., Loza-Reyes, E., Lucas, J., Hammond-Kosack, K.E. et al. (2011) Analysis of two in planta expressed LysM effector homologs from the fungus *Mycosphaerella graminicola* reveals novel functional properties and varying contributions to virulence on wheat. *Plant Physiology*, 156, 756–769.
- McDonald, M.C., McGinness, L., Hane, J.K., Williams, A.H., Milgate, A. & Solomon, P.S. (2016) Utilizing gene tree variation to identify candidate effector genes in *Zymoseptoria tritici*. G3: Genes, Genomes, Genetics, 6, 779–791.
- McDonald, M.C., Renkin, M., Spackman, M., Orchard, B., Croll, D., Solomon, P.S. et al. (2019) Rapid parallel evolution of azole fungicide resistance in Australian populations of the wheat pathogen *Zymoseptoria tritici*. *Applied and Environmental Microbiology*, 85, e01908-18.
- McDonald, M.C., Taranto, A.P., Hill, E., Schwessinger, B., Liu, Z., Simpfendorfer, S., et al. (2019) Transposon-mediated horizontal transfer of the host-specific virulence protein ToxA between three fungal wheat pathogens. *mBio*, 10, e01515-19.
- Meile, L., Croll, D., Brunner, P.C., Plissonneau, C., Hartmann, F.E., McDonald, B.A. et al. (2018) A fungal avirulence factor encoded in a highly plastic genomic region triggers partial resistance to *Septoria tritici* blotch. *New Phytologist*, 219, 1048–1061.
- Möller, M., Habig, M., Freitag, M. & Stukenbrock, E.H. (2018) Extraordinary genome instability and widespread chromosome rearrangements during vegetative growth. *Genetics*, 210, 517–529.
- O'Driscoll, A., Kildea, S., Doohan, F., Spink, J. & Mullins, E. (2014) The wheat-*Septoria* conflict: a new front opening up? *Trends in Plant Science*, 19, 602–610.
- Orton, E.S., Deller, S. & Brown, J.K.M.M. (2011) *Mycosphaerella graminicola*: from genomics to disease control. *Molecular Plant Pathology*, 12, 413–424.
- Palma-Guerrero, J., Ma, X., Torriani, S.F.F., Zala, M., Francisco, C.S., Hartmann, F.E. et al. (2017) Comparative transcriptome analyses in *Zymoseptoria tritici* reveal significant differences in gene expression among strains during plant infection. *Molecular Plant-Microbe Interactions*, 30, 231–244.
- Parlevliet, J.E. (1979) Components of resistance that reduce the rate of epidemic development. *Annual Review of Phytopathology*, 17, 203–222.
- Perron, H., Jouvin-Marche, E., Michel, M., Ounanian-Paraz, A., Camelo, S., Dumon, A. et al. (2001) Multiple sclerosis retrovirus particles and recombinant envelope trigger an abnormal immune response in vitro, by inducing polyclonal V $\beta$ 16 T-lymphocyte activation. *Virology*, 287, 321–332.
- Pertea, M., Pertea, G.M., Antonescu, C.M., Chang, T.-C., Mendell, J.T. & Salzberg, S.L. (2015) StringTie enables improved reconstruction of a transcriptome from RNA-seq reads. *Nature Biotechnology*, 33, 290–295.
- Poppe, S., Dorsheimer, L., Happel, P. & Stukenbrock, E.H. (2015) Rapidly evolving genes are key players in host specialization and virulence of the fungal wheat pathogen *Zymoseptoria tritici* (*Mycosphaerella graminicola*). *PLoS Pathogens*, 11, e1005055.
- Quevillon, E., Silventoinen, V., Pillai, S., Harte, N., Mulder, N., Apweiler, R. et al. (2005) InterProScan: protein domains identifier. *Nucleic Acids Research*, 33, W116–W120.
- Raymond, C.K., Pownder, T.A. & Sexson, S.L. (1999) General method for plasmid construction using homologous recombination. *BioTechniques*, 26, 134–141.
- Robinson, M.D., McCarthy, D.J. & Smyth, G.K. (2010) edgeR: a Bioconductor package for differential expression analysis of digital gene expression data. *Bioinformatics*, 26, 139–140.
- Rudd, J.J., Kanyuka, K., Hassani-Pak, K., Derbyshire, M., Andongabo, A., Devonshire, J. et al. (2015) Transcriptome and metabolite profiling of the infection cycle of *Zymoseptoria tritici* on wheat reveals a biphasic interaction with plant immunity involving differential pathogen chromosomal contributions and a variation on the hemibiotrophic lifestyle definition. *Plant Physiology*, 167, 1158–1185.
- Sánchez-Vallet, A., McDonald, M.C., Solomon, P.S. & McDonald, B.A. (2015) Is *Zymoseptoria tritici* a hemibiotroph? *Fungal Genetics and Biology*, 79, 29–32.
- Selker, E.U. (2002) Repeat-induced gene silencing in fungi. *Advances in Genetics*, 46, 439–450.

- Sexton, A.C. & Howlett, B.J. (2001) Green fluorescent protein as a reporter in the *Brassica-Leptosphaeria maculans* interaction. *Physiological and Molecular Plant Pathology*, 58, 13–21.
- Solomon, P.S., Thomas, S.W., Spanu, P., Oliver, R.P. (2003) The utilisation of di/tripeptides by *Stagonospora nodorum* is dispensable for wheat infection. *Physiological and Molecular Plant Pathology*, 63, 191–199.
- Sperschneider, J., Dodds, P.N., Gardiner, D.M., Singh, K.B. & Taylor, J.M. (2018) Improved prediction of fungal effector proteins from secretomes with EffectorP 2.0. *Molecular Plant Pathology*, 19, 2094–2110.
- Sperschneider, J., Gardiner, D.M., Dodds, P.N., Tini, F., Covarelli, L., Singh, K.B. et al. (2016) EffectorP: Predicting fungal effector proteins from secretomes using machine learning. *New Phytologist*, 210, 743–761.
- Sprouffske, K. & Wagner, A. (2016) Growthcurver: an R package for obtaining interpretable metrics from microbial growth curves. *BMC Bioinformatics*, 17, 172.
- Stamatakis, A. (2014) RAxML version 8: a tool for phylogenetic analysis and post-analysis of large phylogenies. *Bioinformatics*, 30, 1312–1313.
- Stewart, E.L., Croll, D., Lendenmann, M.H., Sanchez-Vallet, A., Hartmann, F.E., Palma-Guerrero, J. et al. (2017) Quantitative trait locus mapping reveals complex genetic architecture of quantitative virulence in the wheat pathogen *Zymoseptoria tritici*. *Molecular Plant Pathology*, 19, 201–216.
- Stewart, E.L. & McDonald, B.A. (2014) Measuring quantitative virulence in the wheat pathogen *Zymoseptoria tritici* using high-throughput automated image analysis. *Phytopathology*, 104, 985–992.
- Suffert, F., Ravigné, V. & Sachec, I. (2015) Seasonal changes drive short-term selection for fitness traits in the wheat pathogen *Zymoseptoria tritici*. *Applied and Environmental Microbiology*, 81, 6367–6379.
- Suffert, F., Sache, I. & Lannou, C. (2011) Early stages of Septoria tritici blotch epidemics of winter wheat: build-up, overseasoning, and release of primary inoculum. *Plant Pathology*, 60, 166–177.
- Testa, A.C., Hane, J.K., Ellwood, S.R. & Oliver, R.P. (2015) CodingQuarry: highly accurate hidden Markov model gene prediction in fungal genomes using RNA-seq transcripts. *BMC Genomics*, 16, 170.
- Thomas, S.R. & Elkinton, J.S. (2004) Pathogenicity and virulence. *Journal of Invertebrate Pathology*, 85, 146–151.
- Tiley, A.M.M., White, H.J., Foster, G.D. & Bailey, A.M. (2019) The *ZtvelB* gene is required for vegetative growth and sporulation in the wheat pathogen *Zymoseptoria tritici*. *Frontiers in Microbiology*, 10, 2210.
- Torriani, S.F.F., Melichar, J.P.E., Mills, C., Pain, N., Sierotzki, H. & Courbot, M. (2015) *Zymoseptoria tritici*: A major threat to wheat production, integrated approaches to control. *Fungal Genetics and Biology*, 79, 8–12.
- Vaser, R., Sović, I., Nagarajan, N. & Šikić, M. (2017) Fast and accurate *de novo* genome assembly from long uncorrected reads. *Genome Research*, 27, 737–746.
- Walker, B.J., Abeel, T., Shea, T., Priest, M., Abouelliel, A., Sakthikumar, S. et al. (2014) Pilon: An integrated tool for comprehensive microbial variant detection and genome assembly improvement. *PLoS One*, 9, e112963.
- Wicker, T., Sabot, F., Hua-Van, A., Bennetzen, J.L., Capy, P., Chalhoub, B. et al. (2007) A unified classification system for eukaryotic transposable elements. *Nature Reviews Genetics*, 8, 973–982.
- Yang, N., McDonald, M.C., Solomon, P.S. & Milgate, A.W. (2018) Genetic mapping of *Stb19*, a new resistance gene to *Zymoseptoria tritici* in wheat. *Theoretical and Applied Genetics*, 131, 2765–2773.
- Zhong, Z., Marcel, T.C., Hartmann, F.E., Ma, X., Plissonneau, C., Zala, M. et al. (2017) A small secreted protein in *Zymoseptoria tritici* is responsible for avirulence on wheat cultivars carrying the *Stb6* resistance gene. *New Phytologist*, 214, 619–631.

## SUPPORTING INFORMATION

Additional Supporting Information may be found online in the Supporting Information section.

**How to cite this article:** Wang C, Milgate AW, Solomon PS, McDonald MC. The identification of a transposon affecting the asexual reproduction of the wheat pathogen *Zymoseptoria tritici*. *Mol Plant Pathol*. 2021;22:800–816. <https://doi.org/10.1111/mpp.13064>